Mechanical and morphological properties of uniaxially oriented and heat-treated poly(lactic acid)/poly(butylene adipate-co-terephthalate) blends

Csézi G., Tábi T.

Accepted for publication in Advances in Polymer Technology
Published in 2025
DOI: 10.1155/adv/7082244

Wiley
Advances in Polymer Technology
Volume 2025, Article ID 7082244, 11 pages
https://doi.org/10.1155/adv/7082244

WILEY

Research Article

Mechanical and Morphological Properties of Uniaxially Oriented and Heat-Treated Poly(Lactic Acid)/Poly(Butylene Adipate-Co-Terephthalate) Blends

Gergely Csézi [1,2] **and Tamás Tábi** [2]

[1]*HUN-REN-BME Research Group for Composite Science and Technology, Műegyetem rkp. 3, H-1111, Budapest, Hungary*
[2]*Department of Polymer Engineering, Faculty of Mechanical Engineering, Budapest University of Technology and Economics, Műegyetem rkp. 3., H-1111, Budapest, Hungary*

Correspondence should be addressed to Tamás Tábi; tabi@pt.bme.hu

Received 27 February 2025; Accepted 26 May 2025

Academic Editor: Puyou Jia

This paper investigates the effect of poly(butylene adipate-co-terephthalate) (PBAT) on the mechanical and morphological properties of poly(lactic acid) (PLA) when the PLA is blended with 10%, 20%, and 30% PBAT and subjected to different draw ratios (DRs), followed by annealing at a fixed length. Results indicate that PBAT functions more as a strengthening agent than a toughening agent when the blend is drawn. Furthermore, both undrawn and most drawn samples exhibit higher crystallinity and lower cold crystallization temperatures (T_{cc}) (in proportion to PBAT ratio) compared to the unblended material, with crystallinity equilibrating at the highest measured draw ratio (DR) of 4, as determined by differential scanning calorimetry (DSC). The crystallinity of the annealed samples equilibrates at 45%–47%, demonstrating the effectiveness of heat treatment at the cold crystallization temperatures of the samples, as measured by DSC, which decreases with increasing DR. However, X-ray diffraction (XRD) results show that heat treatment at the original T_{cc}, specific to the undrawn PLA, results in higher crystal orientation.

Keywords: biopolymer; drawing; orientation; poly (butylene adipate-co-terephthalate) blend; poly(lactic acid); poly(lactic acid) blend

1. Introduction

Nowadays, the most frequent materials that surround us are different kinds of plastics, regardless of whether the product is for long-term use or short-term use. Due to the low prices of the neat materials, their low processing cost, and their versatility, polymer production per annum has increased for decades, except in 2020, when there was a constancy (at 380 Mt), due to the COVID-19 pandemic. However, plastic waste increased sharply due to protective measures such as masks and gloves or single-use plastic bags. This increasing amount of plastic worldwide is causing more and more infrastructural problems with waste [1, 2]. Landfills only offer a short-term solution, which is now untenable. Incinerators can be a solution, with precise regulation and filters, but they produce carbon dioxide. Recycling seemed the most promising way. Unfortunately, compared with the price of fresh, first-cycle plastic prices, recycling is an expensive and complicated procedure (collecting, transferring, selecting, and cleaning), which, without regulation, is only an opportunity [3, 4]. Reuse and recycling both occur in the circular economy, meaning we would rather repair a used product or make a new product from the material by mechanical or chemical recycling than dispose of them [5]. After bio-based and biologically degradable thermoplastics appeared with rationally low cost and wide availability, it is clear, that this could be the best material group to fit in the circular economy. As thermoplastics, they could also be recycled in the same way as petroleum-based plastics, but being biodegradable means it could also be composted, degrading to only natural traces [6, 7].

In the late ’80s, Cargill Inc. started a project to make poly (lactic acid) (PLA) from renewable resources. They developed a

key process to make high molecular weight PLA from starch. Earlier, even if the PLA was known and used in medical applications (surgery), it was too expensive to hit the market to be used as a material for simpler products. The project was successful, and in 2001, they managed to produce 140,000 metric tons of PLA per year and this amount continued to increase [8]. As a bio-based and biodegradable polymer, it can be easily adjusted to the circular economy. PLA is a thermoplastic, aliphatic polyester built up from the two stereoisomers of lactic acid (D- and L-lactic acid) as a copolymer. The ratio of these two units determines the properties of the polymer. If the polymer is built up from only one isomer, it is isotactic. The available PLAs in the market contain approximately0.5%–15% D-lactic acid. The lower the D-lactic acid content, the higher the crystalline ratio, but over approximately 10%, the PLA is totally amorphous. The glass transition temperature (T_g) of PLA is about 50°C–60°C, and the melting temperature (T_m) is 135°C–180°C, depending on the ratio of the lactic acids. The lower the D-lactic acid content, the higher the T_g and T_m. On the other hand, PLA has a tensile strength of around 45–60 MPa, a tensile modulus of around 3500–4000 MPa, and elongation at a break of around 3%–6% [9, 10]. From the above properties, it is clear that the most significant application drawbacks are the low T_g, the low heat deflection temperature (HDT), and the low elongation at break. The HDT can be increased with a higher crystalline ratio, which could be obtained by annealing after processing or during processing by using nucleating agents along with in-mold crystallization [11–13]. An increasing number of papers focusing on orienting PLA highlighted that drawing PLA films between the glass transition temperature and the cold crystallization temperature (T_{cc}) can increase the T_g of the polymer [14, 15]. To reach higher elongation at break, one can also use the benefits of orientation, as it also enhances elongation and thus, toughness. Another way to reach higher elongation at break is to blend PLA with other inherently tough polymers or plasticizers, like natural rubber (NR), poly (butylene adipate terephthalate) (PBAT), poly (butylene succinate) (PBS), etc., but they could also affect the kinetics of crystallization [16–22]. A combination of blending and orientation of PLA and PBAT was investigated by Zhang et al. [19]. They found that forming oriented molecular chains of PLA is hard when PBAT content is above 30%, but below that, they sSuccessfully reinforced and toughened PLA with a drawing speed of 25 mm/min and a draw ratio (DR) of 4 at a temperature of 80°C. Due to the lack of citations about PLA/PBAT blends and also the lack of examination of the drawing parameters, such as DR, the main purpose of this article is to investigate the effect of the different draw ratios (DRs) on the distinct mixing ratios of PLA/PBAT blends.

2. Experimental

2.1. Materials and Processing. The extrusion grade PLA type 4032D with a D-lactide content of 1.4% was purchased from Natureworks (Minnetonka, MN) (the D-lactide content was provided by the manufacturer). The PBAT (ecoFlex F Blend 1200) was purchased from BASF (Ludwigshafen, Germany). Prior to processing, we mixed PLA and PBAT pellets in the ratio of 90/10, 80/20, and 70/30, then dried the mixtures in a hot air drier at 80°C for 8 h to remove moisture, before we compounded the blends from the mixture with twin screw extruder (LabTech LTE 26-44) to make filaments, then pellets. The extruder was equipped with a 26 mm diameter screw with an L/D ratio of 44, and zone temperatures were set to 190°C, 190°C, 185°C, 185°C, 185°C, 180°C, 180°C, 180°C, 175°C, 175°C, and 175°C (from die to hopper). Screw rotation speed was 20 1/min. The 0.5 mm thick sheets were made with a Labtech LCR 300 film sheet extruder (screw diameter 25 mm, L/D = 30) equipped with a slit die set to a slit distance of 0.8 mm. The temperature of the chill roll was set to 60°C, and the pulling speed was 0.9 m/min. The extrusion temperatures were 190°C, 185°C, 180°C, 175°C, and 175°C (from die to hopper) and screw rotation speed was 54 1/min. After extrusion, dumbbell-shaped specimens were cut from the sheets for drawing. After orientation, we cooled the dumbbell-shaped samples down to ambient temperature fast to avoid relaxation. To also avoid the effects of physical aging in mechanical properties, we waited 3 days before further tests after the orientation and heat treatments. We performed the heat treatments in the heat chamber, with the sample fixed to a frame longitudinally, to avoid shrinkage of the samples.

2.2. Methods. We drew the samples with a Zwick Z250 universal testing machine (Ulm, Germany) equipped with a Zwick BZ 005/TN2S force-measuring cell with a force limit of 5 kN. The machine was equipped with a heat chamber. Drawing temperature was set to 70°C, and for the first drawing, we waited for 1 h for the chamber to heat up and then waited 3 min after each specimen we took in to warm up. Grip-to-grip separation was set to 20 mm, and the cross-head speed was 144 mm/min, so the Hencky strain rate was 0.12 1/s. The final DRs) were 1, 1.5, 2, 3, and 4. Five independent tests were carried out for each parameter set.

Scanning Electron Microscopy (SEM) were carried out with a JEOL JSM 6380LA from (Jeol Ltd., Japan, Tokyo) after the samples were broken cryogenically in liquid nitrogen parallel to the extrusion and drawing direction and coated with a gold layer.

We measured thermal and crystallization properties by differential scanning calorimetry (DSC) with device from TA Instruments (Q2000). The 4–6 mg samples were tested in 50 mL/min nitrogen purge gas from 0 to 200°C, with a heating rate of 5°C/min, modulated with ±1°C/min. We determined the glass transition temperature (T_g), cold crystallization temperature (T_{cc}), the enthalpy of cold crystallization (ΔH_{cc}) and melting (ΔH_m), and melting temperature (T_m). Crystallinity was calculated with Equation (1):

$$X_c = \frac{\Delta H_m - \Delta H_{cc}}{\Delta H_f \cdot (1-\alpha)} \cdot 100\,(\%)(1),$$

where X (%) is the calculated crystallinity, ΔH_m (J/g) and ΔH_{cc} (J/g) are the enthalpy of fusion and the enthalpy of cold crystallization, respectively, while ΔH_f (J/g) is the enthalpy of fusion for 100% crystalline PLA (93.0 J/g) and α is the ratio of the other phase.

Table 1: Grip-to-grip separations and test speeds of the different draw ratios.

Drawing ratio	Grip-to-grip separation (mm)	Test speed (mm/min)
DR1	20	2
DR1.5	35	2
DR2	45	5
DR3	65	5
DR4	85	5

Note: DR1 means that the sample was not drawn at all. DR1.5 means a drawing ratio of 1.5. DR2 means a drawing ratio of 2. DR3 means a drawing ratio of 3. DR4 means a drawing ratio of 4.

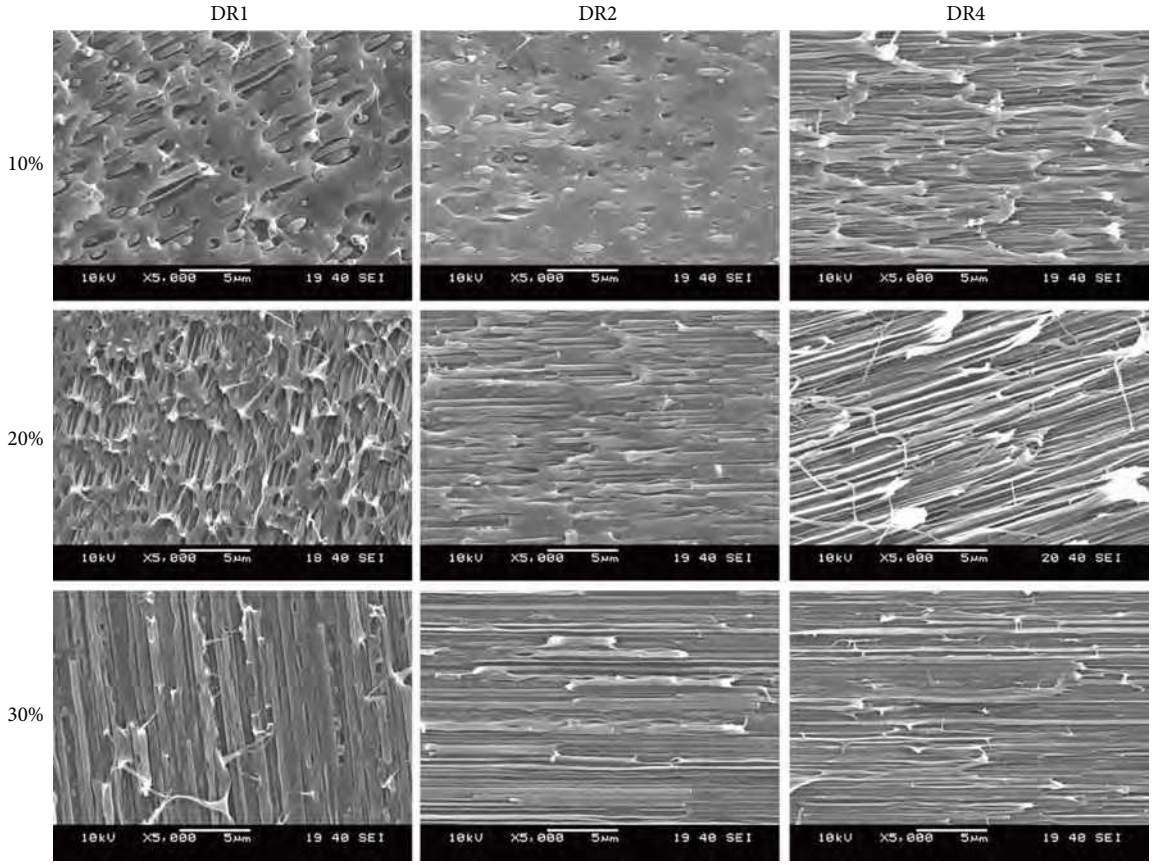

Figure 1: SEM images of the samples containing 10%–30% PBAT undrawn and with a draw ratio of 2 and 4.

From the DSC results, we selected the annealing temperatures for the different blends to be the same as their T_{cc} temperatures, then half of the samples were annealed with a fixed length, and the other half were tensile tested without heat treatment.

X-Ray diffraction (XRD) was performed with an X'Pert Pro MPD device from PANalytical (Almelo, Netherlands). The patterns were obtained from 5° to 40° (2θ). The type of the detector was X'celerator. Radiation was Cu Kα with an Ni filter foil ($\lambda = 1.5408$ Å), and the sample holder was a Si single crystal.

The tensile tests were performed on a Zwick Z005 universal testing machine (Ulm, Germany) equipped with a 5 kN force cell. As the samples were drawn to different DRs, the sample lengths were different, so for equal strain rates during the test, we used different cross-head speeds, previously calibrated with the different sample geometries. The final grip-to-grip separation and test speed for the different DRs are shown in Table 1.

3. Results and Discussion

After drawing, the longitudinal cryogenic fracture surfaces of the samples were examined by SEM (Figure 1).

From the undrawn samples, as Deng et al. [23] also showed in their article, the blend was co-continuous at 20% and 30%, while at 10%, PBAT was dispersed as droplets in the PLA matrix. At DR2, both structures deformed in the direction of orientation. In the sample containing 10% PBAT, the droplets and cavities were transformed into oval shapes, whsile with 20% PBAT content, the branches of the structure faced the

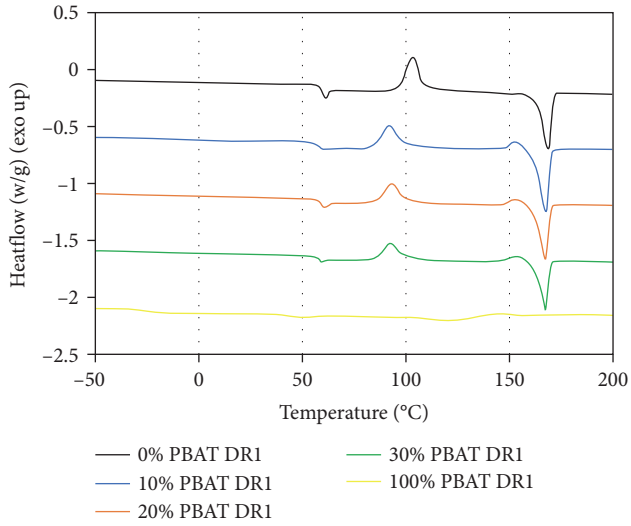

FIGURE 2: DSC curves of undrawn (DR1) PLA/PBAT samples containing 0%, 10%, 20%, 30%, and 100% PBAT.

TABLE 2: The presence of α and α' crystal structure forms in the samples.

PBAT content (in %)	DR				
	1	1.5	2	3	4
0	α'	α'	α'	α'	α
10	α'	α'	α'	α' + α	α
20	α'	α'	α'	α' + α	α
30	α'	α'	α'	α' + α	α

drawing direction. With 30% PBAT, drawing only made the branches thinner, as the undrawn sample preserved more of the orientation from extrusion. At DR4, as orientation increased, the shape of the droplets in the sample with 10% PBAT looked like the branches in the samples containing 20% and 30% PBAT, but with lower orientation. In the samples containing 20% and 30% PBAT, the structures look the same as with DR2, but the branches are thinner. However, there are also some noticeable differences with DR4. The oriented branches seem thinner and finer, so the PBAT may have a greater specific surface area, which can cause changes in the PLA's crystalline structure.

After SEM, we performed DSC. The undrawn PLA/PBAT blend samples DSC curves, containing 0%, 10%, 20%, 30%, and 100% PBAT are shown in Figure 2.

Figure 3 shows the DSC curves of the samples containing 10% PBAT, but drawn to different DRs.

The tendency of the other samples DSC curves with the same DR, but different PBAT content are similar, so the differences will be shown in diagrams for better description. However, as Figure 3 shows, drawing increases the glass transition temperature, lowers the cold crystallization temperature, and around the crystal melting temperature, there are some interesting parts, showing that different DRs produce different internal crystalline structures in PLA. These results are summarized in Table 2.

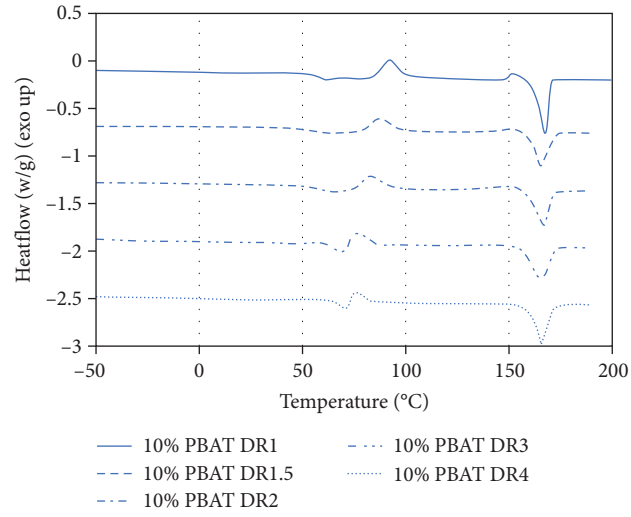

FIGURE 3: DSC curves of samples containing 10% PBAT drawn with different draw ratios.

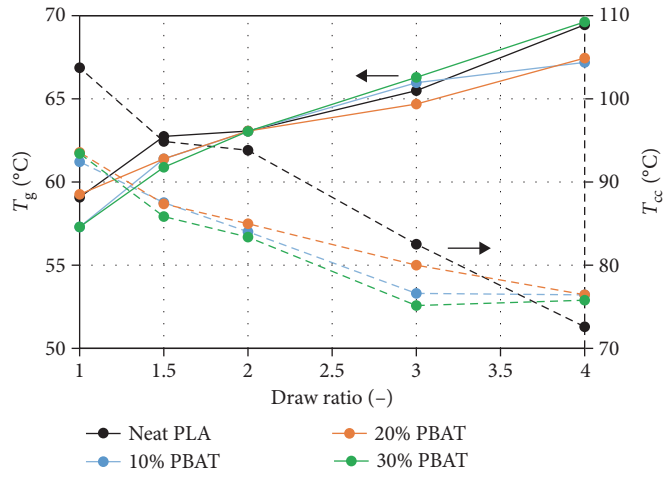

FIGURE 4: Glass transition and cold crystallization temperature of the drawn, nonannealed samples as a function of draw ratio.

In the table, blue color means the sample had a crystal perfection peak before crystal melting, suggesting the α' crystal form, while white means there was no perfection. It seems that PBAT (independently of the amount) in the range of 10% to 30%, and with DR3, results in both α and α' stable forms with no perfection in all the samples, while the sample that does not contain PBAT still only has the nonstable α' form. DR4 produced stable α crystals in all the samples.

As Figure 4 shows, the glass transition temperature of the nonannealed samples (T_g) in this mixing range (0–30 m% PBAT content) was not affected significantly by the PBAT, only by the orientation. Stretching to a DR of 4, increased the material's T_g by approximately 10°C.

The cold crystallization temperature decreases in PLA with an increasing DR due to the higher molecular orientation, which induces the crystallization (Figure 4). However, PBAT also lowers the cold crystallization temperature by accelerating the PLA's crystallization rate [16]. These two phenomena appear

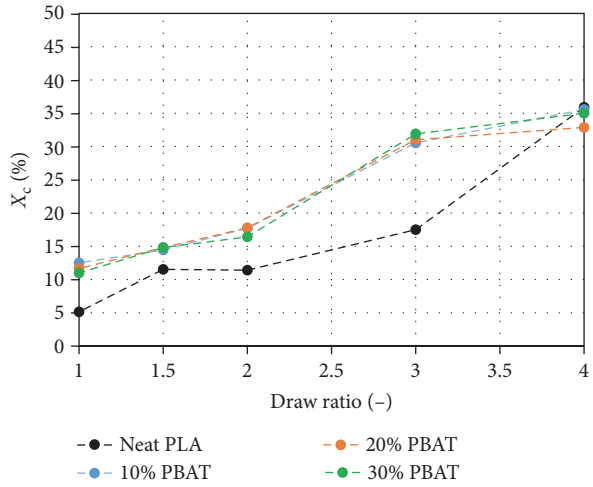

FIGURE 5: PLA's crystalline ratio of the nonannealed drawn samples as a function of draw ratio.

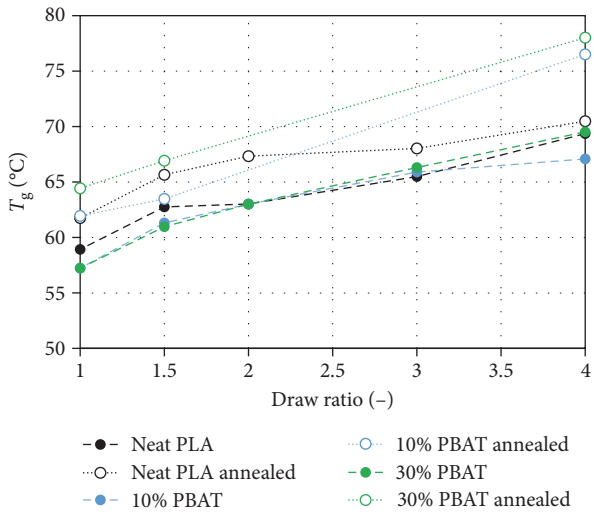

FIGURE 6: Glass transition temperature of the drawn, heat-treated samples as a function of draw ratio.

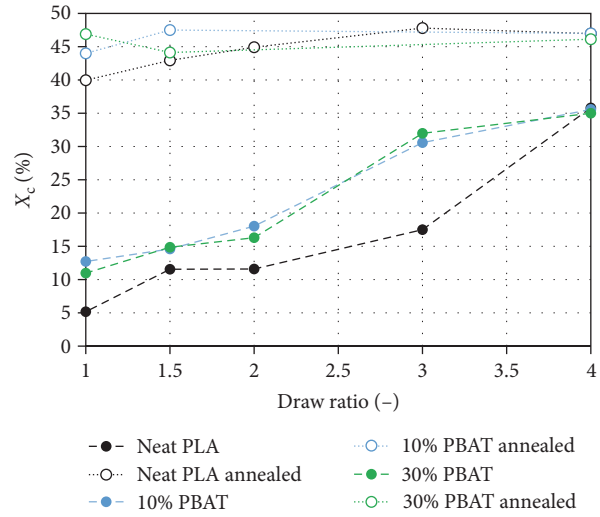

FIGURE 7: DSC curves of oriented PLA samples containing 30% PBAT drawn to different draw ratios.

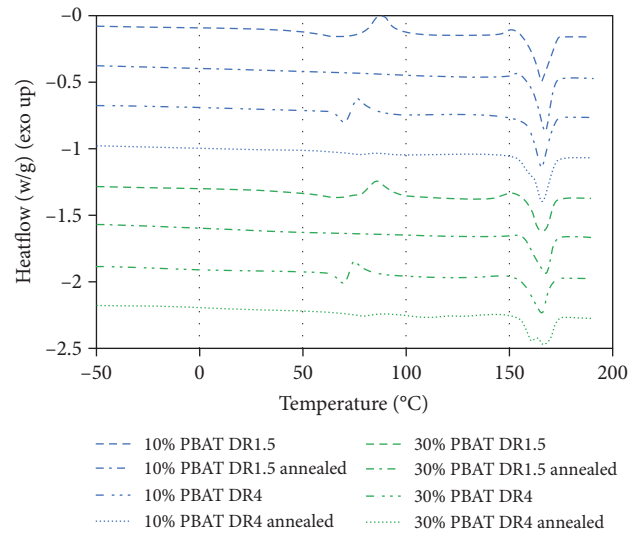

FIGURE 8: Crystalline ratio of the heat-treated drawn samples as a function of draw ratio.

simultaneously in the blended and oriented samples, but with an increasing DR, the difference disappears. It is because cold crystallization temperature has a lower limit, the glass transition temperature, which increases due to orientation, and these two temperatures meet around 70°C (Figure 3 bottom curve).

Similar to the cold crystallization temperature of the samples (Figure 4), the lower the T_{cc} is, the higher the crystalline fraction is. With the highestDR, the crystalline fractions also equilibrated (Figure 5).

Through annealing the samples for 10 min at their T_{cc}, obtained from the DSC results of the nonannealed samples, the T_g can be further increased. A higher PBAT content resulted in a higher T_g, and at the highest DR, 4, the glass transition temperature of the blended samples with heat treatment reached 77°C–78°C (Figure 6), and the cold crystallization peak disappeared (Figure 7).

The effect of annealing on the crystalline ratio was nearly independent of the DR or PBAT content and resulted in a 45% crystalline ratio with every parameter set (Figure 8).

Drawing, PBAT content and the heat treatment also affected the crystalline structure (Figure 7, Table 3).

While with DR1 and DR1.5, annealing only increased crystallinity, and eliminated the thermal relaxation in the DSC curves, but in the case of DR4, α' also appeared after the heat treatment, whereas the sample only contained the α crystal form when unannealed.

XRD was also carried out to show the crystalline structures (Figure 9).

We obtained one main peak at 16–17°, which is specific to the α and α' phase of the PLA, and a small peak around 23°, which is specific to PBAT. The greatest intensity belongs to the blend containing 20% PBAT, drawn to DR4. With DR2, the

Table 3: The presence of α and α' crystal forms in the annealed and nonannealed samples.

PBAT content (in %)	Drawing ratio		
	1	1.5	4
0			
Original	α'	α'	α
Annealed	α'	α'	α' + α
10			
Original	α'	α'	α
Annealed	α'	α'	α' + α
30			
Original	α'	α'	α
Annealed	α'	α'	α' + α

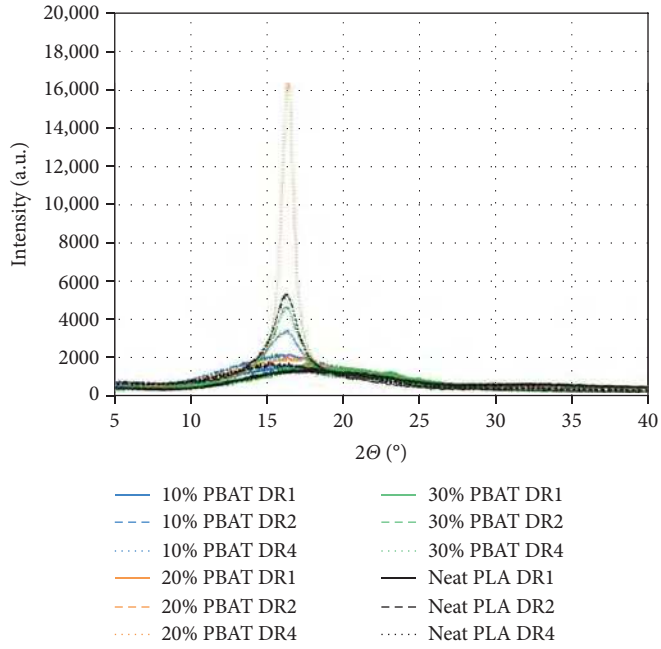

Figure 9: X-ray diffraction intensities as a function of 2Θ° with nonannealed samples.

peaks are low, flat, and wide; the height difference is caused mainly by the difference in the baseline.

The sample with 20% PBAT has the highest peak at DR4, even though all the DR4 samples have the same crystallinity as shown by DSC. It may confirm what we suggested from the SEM images, that this sample has enough PLA, and also a high specific surface area on the PBAT branches, to crystallize perpendicularly. Therefore, even if the crystalline ratio is the same, there can be more crystals in the same direction. Adding 10% PBAT lowers the peak between 16° and 17° compared to the neat PLA at DR4, due to the spherical crystallization around the PBAT droplets. With a PBAT ratio of 30%, the surface area of the PBAT is not higher, but the sample contains less PLA than the sample with 20% PBAT.

Heat treatment caused a rapid rise in the peaks, and also one more peak appeared at 28.7°, which is specific to the α phase of the PLA (Figure 10). With neat PLA and with 30% PBAT, the pattern was the same: the peak was higher when the DRwas 2, not 4. The main reason is that the heat treatment was applied at different temperatures, as DSC showed (Figure 4). After annealing at the same temperatures, the peaks were totally temperature-dependent and not DR–dependent in the case of the blends, but the peak of the neat PLA sample drawn to DR4 and annealed at 95°C did not reach the peak of the DR2 sample annealed at 95°C, but still higher than the peak of the DR4 sample (Figure 11).

This suggests that the decreasing cold crystallization peak temperature seen in the DSC curves is at least partly induced by shrinkage that starts above the glass transition temperature and induces crystallization. However, when the samples are heat-treated, fixing the sample longitudinally prevents this shrinkage in the fixing frame, so XRD shows higher peaks at 95°C. Nevertheless, the DR2 samples annealed at 95°C did not have a higher crystalline fraction than the DR4 samples annealed at 75°C.

The tensile tests showed the effects of drawing and the increasing PBAT content on the mechanical properties of the PLA blend samples (Figures 12 and 13). Stress–strain curves show how the effects of the above were different, and later will be described in more detail.

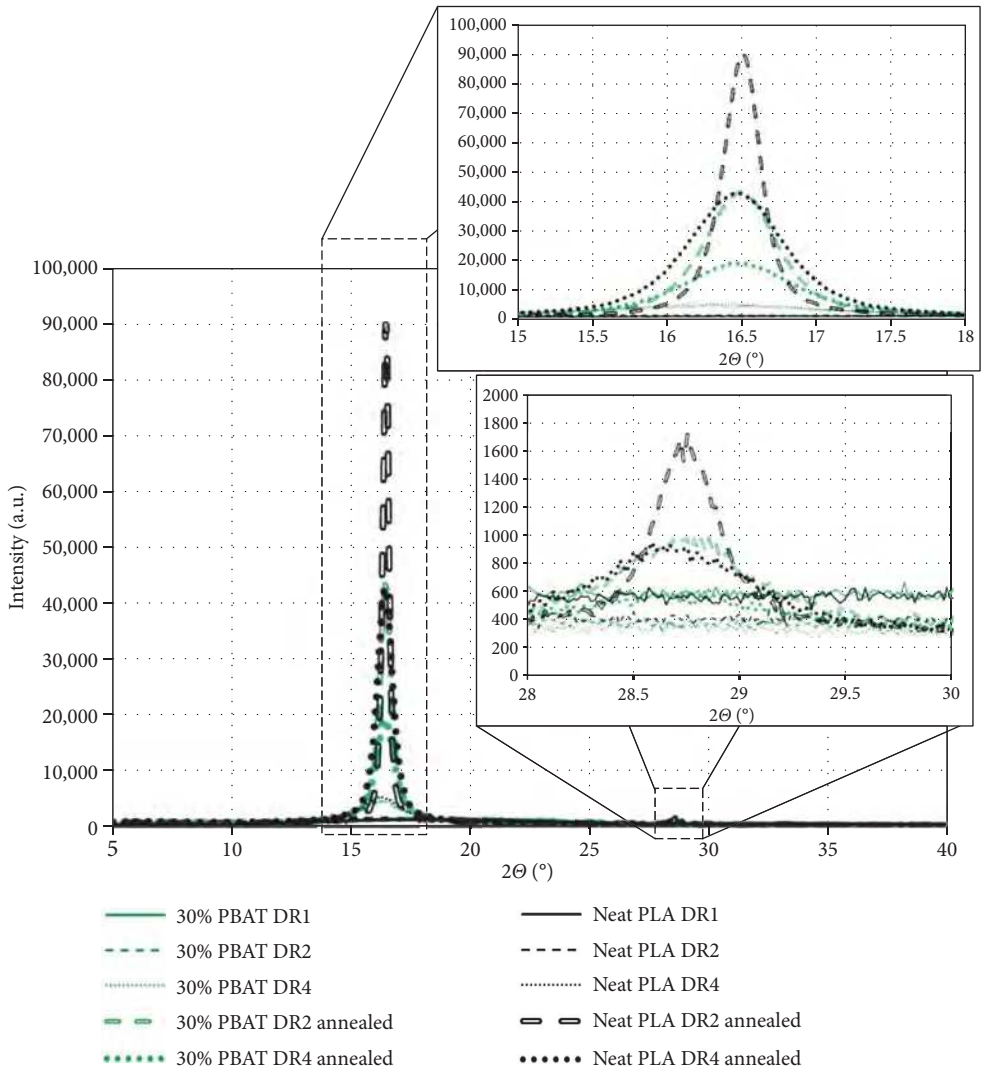

FIGURE 10: X-ray diffraction intensities as a function of $2\Theta°$ with nonannealed and annealed samples.

In the tensile tests of the samples, the oriented samples showed increasing yield strength with increasing DR, compared with the undrawn samples (Figure 14). Up to DR3, only the samples with 10% and 20% PBAT had higher yield strength than neat PLA when drawn, but an increase in PBAT content lowered yield stress.

Unfortunately, heat treatment decreased the yield stress in all samples, and this decrease also depended on the PBAT ratio (Figure 14). An increase in PBAT content lowered the yield stress, and the higher the DR was, the higher the drop was.

The tensile strength of the samples also increased with the DR (Figure 15). Without drawing, PBAT in the PLA lowered the PLA's tensile strength from approximately 55 to 33–40 MPa. The strength of the undrawn and DR1.5 samples that contain PBAT were lower than the samples without PBAT. But above DR1.5, the samples with 10% and 20% PBAT had higher strength than the neat PLA samples with the same DR. The strength of PLA with 30% PBAT was still sligthly under that of the neat PLA. At DR4, the tensile strength of 30% PBAT was similar to that of the other samples, and at that DR, the tensile strengths of the blends were higher than that of the neat PLA.

Annealing only increased tensile strength in the sample with 30% PBAT at DR2 and DR3, and in neat PLA over DR2. In other cases, heat treatment did not increase, and in some cases, slightly decreased strength.

The most interesting results are the strain at break values. Originally, PBAT is used for toughening PLA, and when the samples were not drawn, the PBAT increased the strain of our samples significantly (and decreased tensile strength), but after drawing the samples, the difference between the neat PLA and the blended samples considerably decreased, therefore it seems that drawing strengthens of the PLA-PBAT blends, rather than toughens them (Figure 16).

Interestingly, heat treatment further increased elongation at break in the case of DR3 and 4, and the presence of PBAT boosted that phenomenon, while under DR2, heat treatment made the samples more rigid. The decrement of the strain at break at DR2 and under that depended on the mixing ratio. Smaller PBAT content resulted in a greater decrease.

The work of rupture calculated from the tensile tests (Figure 17) indicate that the most rigid blend from the drawn and not annealed samples were the samples containing 30%

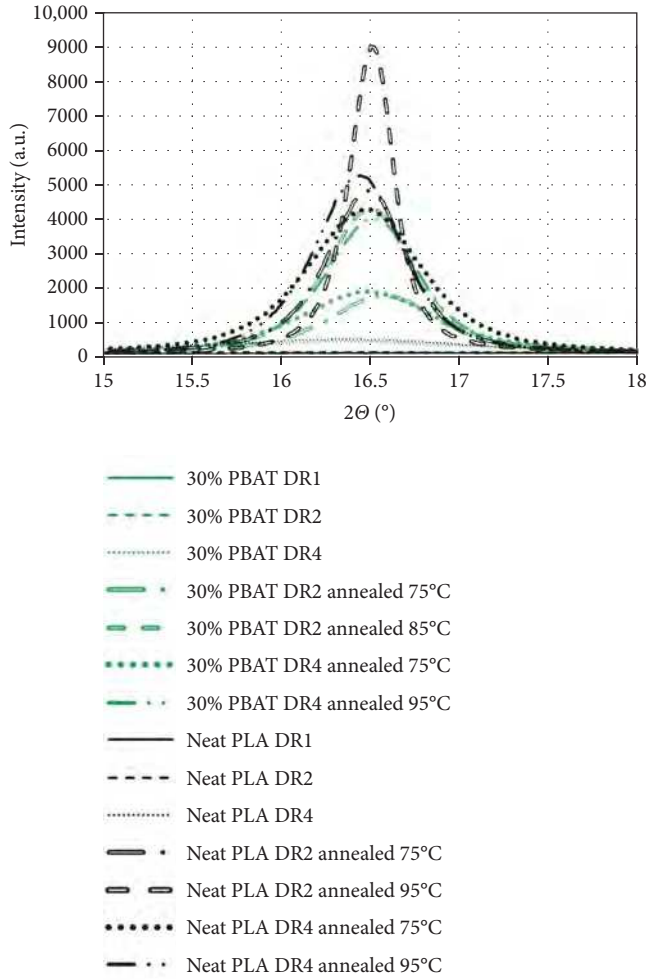

FIGURE 11: X-ray diffraction intensities as a function of $2\Theta°$ with nonannealed and annealed samples in the range of 15°–18° with both heat-treating (HT) temperatures for every sample.

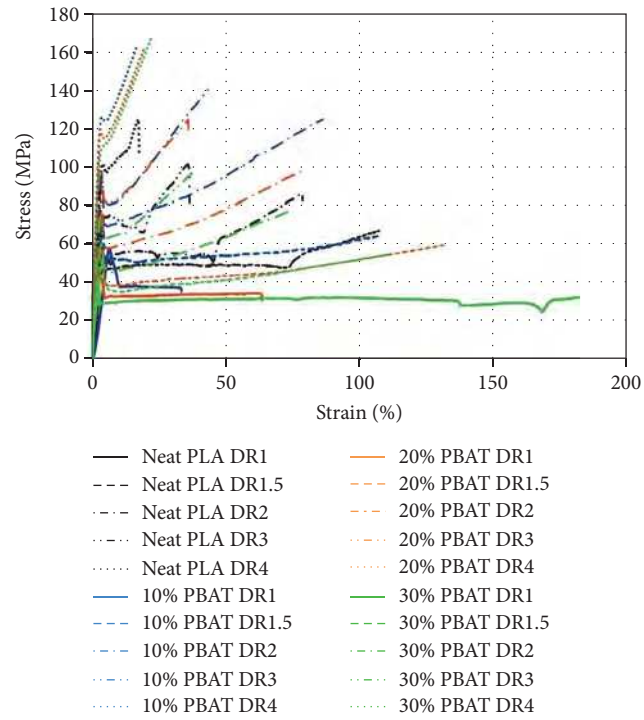

FIGURE 12: Stress–strain curves of the nonannealed samples.

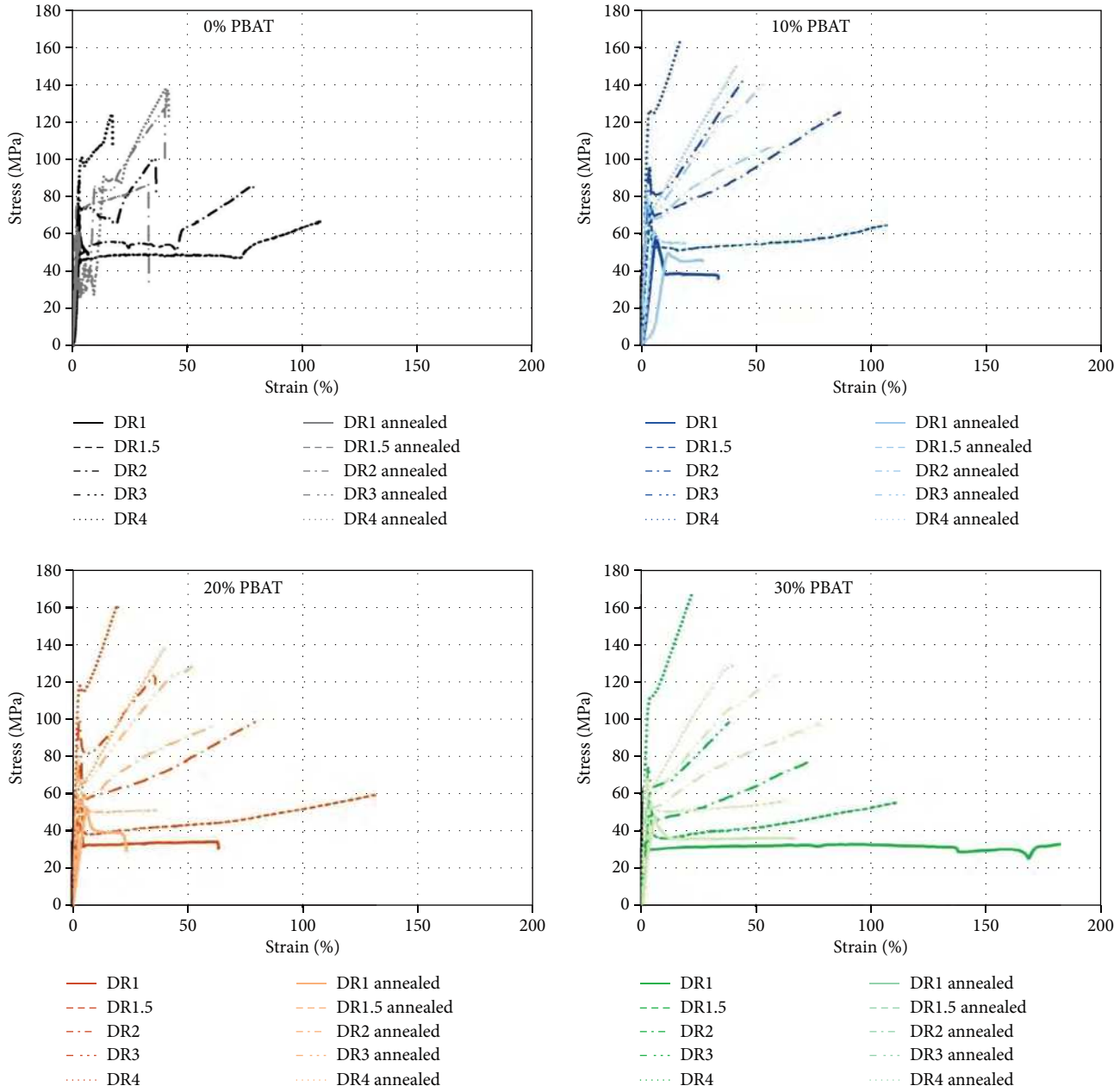

FIGURE 13: Stress–strain curves of the nonannealed and annealed samples separated by the PBAT content.

PBAT, with DRs of 1.5, 2 and 3. On the other hand, this blend's work of rupture changed the least as a function of DR. The effect of annealing on the work of rupture was similar to its effect on strain at break; at DR3 and 4, it further increased toughness, but in inverse proportion to PBAT content.

4. Conclusion

In this article, we investigated the effect of PBAT content (10%, 20%, and 30%), orientation above the glass transition temperature (70°C, no drawing and a DR of 1.5, 2, 3, and 4), and heat treatment (at the cold crystallization temperature) on the mechanical and morphological properties of a PLA film with low D-lactide (1.4%) content. At 20% and 30% PBAT content, the phase structure was co-continuous, and drawing aligned the structure in the direction of drawing. With 10% PBAT, even though the structure was „droplets in the matrix", the structure was so oriented at the highest DR, 4, that it looked co-continuous. DSC showed that drawing decreased the cold crystallization temperature, increased crystallinity and changed the crystalline structure. At the highest DR, crystal perfection disappeared before melting, resulting in a more oriented and ordered crystal structure. Adding PBAT to PLA further increased the crystallinity at every DR, except at the highest, 4, but slightly decreased T_g. The addition of PBAT also affected the crystalline structure. At DR3, α and α' appeared in the same sample. When the samples were annealed, the glass transition temperatures of the blends increased, mainly at the highest

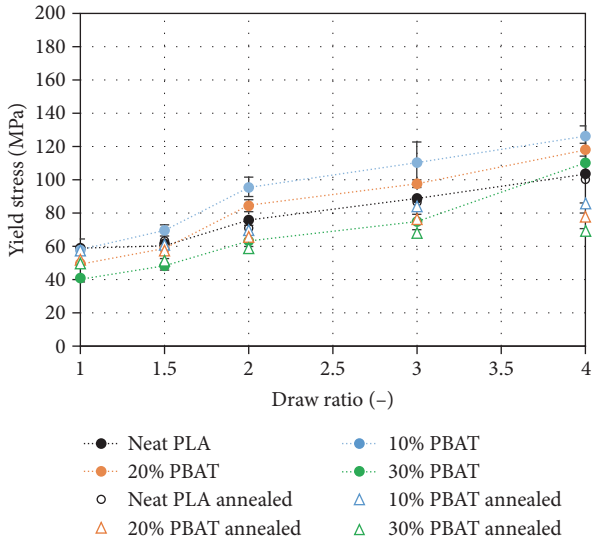

FIGURE 14: Yield stress of the nonannealed and annealed samples as a function of the draw ratio.

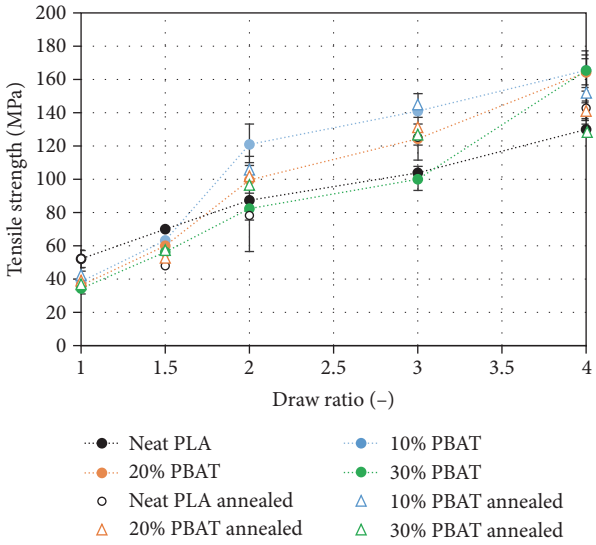

FIGURE 15: Tensile strength of the nonannealed and annealed samples as a function of draw ratio.

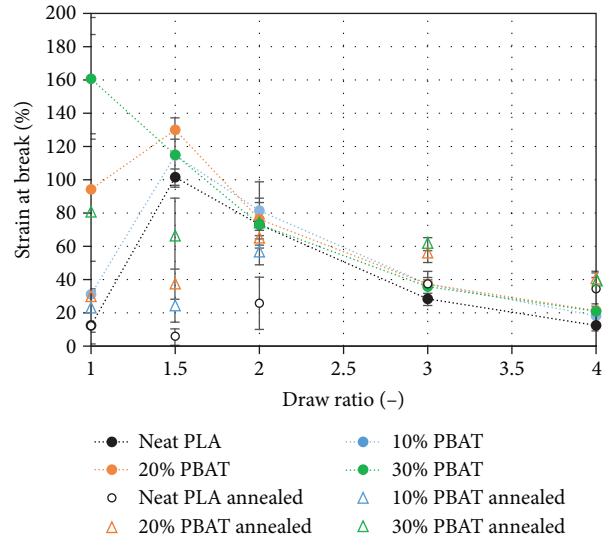

FIGURE 16: Strain at break values of the nonannealed and annealed samples as a function of the draw ratio.

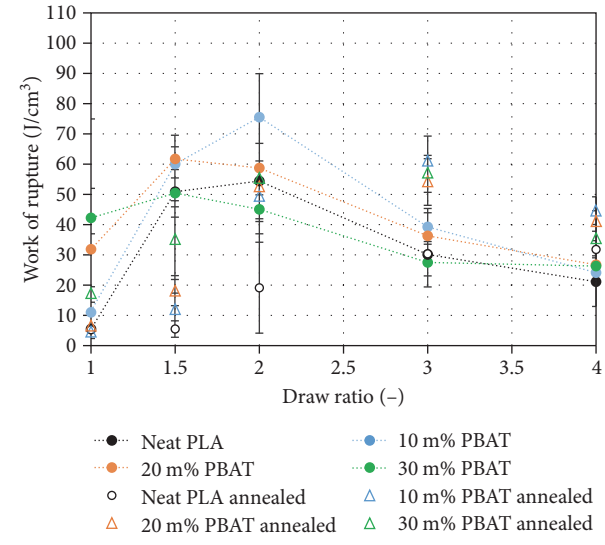

FIGURE 17: Work of rupture of the nonannealed and annealed samples as a function of draw ratio.

DRs, to approximately 76°C–78°C. Independently of the DR and PBAT content, crystallinity increased to 45%–47% after annealing. XRD curves showed the α and α' phase of PLA at $2\Theta = 16–17°$, with the highest peak belonging to the most drawn 20% PBAT-containing samples. This peak may be due to the fact that the 20% PBAT sample had a co-continuous structure, similarly to the 30% PBAT sample, but the 20% PBAT sample had more PLA that could crystallize, therefore the peak was higher. In the case of the annealed samples, all the peaks around $2\Theta = 16°–17°$ got higher, but the DR2 samples were higher than the DR4 samples due to the difference in the heat treatment temperature. All samples were annealed at T_{cc}, characteristic of the DR. T_{cc} is 95°C when the sample is undrawn but is reduced as a result of drawing. However, we also annealed all drawn samples at 95°C as well. As a result of annealing at 95°C, the T_{cc} of the undrawn sample, the peaks became higher and sharper in all cases. Consequently, the orientation of the crystals was higher when annealed at the cold crystallization temperature of the neat, undrawn PLA, but the same crystalline ratio can be achieved with the lower temperature, with a more relaxed structure. PBAT behaved more like a strengthening agent than a toughening agent when the samples were oriented. However, with heat treatment, the toughness of the samples was also further increased when drawn at higher DRs than DR2.

Data Availability Statement

Data are available upon request.

Conflicts of Interest

The authors declare no conflicts of interest.

Author Contributions

Gergely Csézi: methodology, measurements, writing – review and editing, visualization. **Tamás Tábi:** conceptualization, supervision, writing – original draft, project administration, funding acquisition.

Funding

This research was supported by the National Research, Development and Innovation Office (Grant OTKA FK134336), National Research, Development and Innovation Fund (Grant TKP-6-6/PALY-2021), and Programme Széchenyi Plan Plus (Grant RRF-2.3.1-21-2022-00009).

Acknowledgments

This work was supported by the National Research, Development and Innovation Office, Hungary (OTKA FK134336). Project no. TKP-6-6/PALY-2021 has been implemented with the support provided by the Ministry of Culture and Innovation of Hungary from the National Research, Development and Innovation Fund, financed under the TKP2021-NVA funding scheme. Project no. RRF-2.3.1-21-2022-00009, titled National Laboratory for Renewable Energy has been implemented with the support provided by the Recovery and Resilience Facility of the European Union within the framework of Programme Széchenyi Plan Plus.

References

[1] Plastics Europe, "Plastics—The fast Facts 2023," 2024, https://plasticseurope.org/knowledge-hub/plastics-the-fast-facts-2023/.

[2] G. Gorrasi, A. Sorrentino, and E. Lichtfouse, "Back to Plastic Pollution in COVID Times," *Environmental Chemistry Letters* 19, no. 1 (2021): 1–4.

[3] R. Geyer, J. R. Jambeck, and K. L. Law, "Production, Use, and Fate of All Plastics Ever Made," *Science Advances* 3, no. 7 (2017): 1–5.

[4] S. Horváth and J. G. Kovács, "Effect of Processing Parameters and Wall Thickness on the Strength of Injection Molded Products," *Periodica Polytechnica Mechanical Engineering* 68, no. 1 (2024): 78–84.

[5] W. R. Stahel, "The Circular Economy," *Nature* 531, no. 7595 (2016): 435–438.

[6] L. Yu, *Biodegradable Polymer Blends and Composites from Renewable Resources* (John Wiley and Sons Inc, New Jersey, 2009).

[7] T. Tábi, "What Is the Next Step for Bioplastics?" *Express Polymer Letters* 18, no. 11 (2024): 1063-1064.

[8] E. T. H. Vink, K. R. Rábago, D. A. Glassner, and P. R. Gruber, "Applications of Life Cycle Assessment to NatureWorks™ Polylactide (PLA) Production," *Polymer Degradation and Stability* 80, no. 3 (2003): 403–419.

[9] G. Stoclet, R. Séguéla, J. M. Lefebvre, S. Li, and M. Vert, "Thermal and Strain-Induced Chain Ordering in Lactic Acid Stereocopolymers: Influence of the Composition in Stereomers," *Macromolecules* 44, no. 12 (2011): 4961–4969.

[10] S. Saeidlou, M. A. Huneault, H. Li, and C. B. Park, "Poly (Lactic Acid) Crystallization," *Progress in Polymer Science* 37, no. 12 (2012): 1657–1677.

[11] T. Tábi, S. Hajba, and J. G. Kovács, "Effect of Crystalline Forms (α′ and α) of Poly(lactic Acid) on Its Mechanical, Thermo-Mechanical, Heat Deflection Temperature and Creep Properties," *European Polymer Journal* 82 (2016): 232–243.

[12] T. Tábi, A. F. Wacha, and S. Hajba, "Effect of D-Lactide Content of Annealed Poly(Lactic Acid) on Its Thermal, Mechanical, Heat Deflection Temperature, and Creep Properties," *Journal of Applied Polymer Science* 136, no. 8 (2019): 47103.

[13] L. Yu, H. Liu, F. Xie, L. Chen, and X. Li, "Effect of Annealing and Orientation on Microstructures and Mechanical Properties of Polylactic Acid," *Polymer Engineering & Science* 48, no. 4 (2008): 634–641.

[14] M. Razavi and S.-Q. Wang, "Why Is Crystalline Poly(Lactic Acid) Brittle at Room Temperature?" *Macromolecules* 52, no. 14 (2019): 5429–5441.

[15] Y. Chen, L. Zhao, H. Pan, S. Jia, L. Han, and L. Dong, "Impact of d-Isomer Content on the Microstructure and Mechanical Properties of Uniaxially Pre-Stretched Poly(Lactic Acid)," *Polymer* 186 (2020): 122022.

[16] L. Jiang, M. P. Wolcott, and J. Zhang, "Study of Biodegradable Polylactide/Poly(Butylene Adipate-Co-Terephthalate) Blends," *Biomacromolecules* 7, no. 1 (2006): 199–207.

[17] C. Zhang, W. Wang, Y. Huang, et al., "Thermal, Mechanical and Rheological Properties of Polylactide Toughened by Expoxidized Natural Rubber," *Materials & Design* 45 (2013): 198–205.

[18] A. Bhatia, R. K. Gupta, S. N. Bhattacharya, and H. J. Choi, "Compatibility of Biodegradable Poly (Lactic Acid) (PLA) and Poly (Butylene Succinate) (PBS) Blends for Packaging Application," *Korea-Australia Rheology Journal* 19 (2007): 125–131.

[19] T. Zhang, P. Wu, Q. Yang, and J. Jiang, "Fabrication of Reinforced and Toughened Poly(Lactic Acid)/Poly(butylene Adipate-Co-Terephthalate) Composites Through Solid Die Drawing Process," *Journal of Applied Polymer Science* 137, no. 36 (2020): 49071.

[20] J. F. Fatriansyah, E. Kustiyah, S. N. Surip, et al., "Fine-Tuning Optimization of Poly Lactic Acid Impact Strength With Variation of Plasticizer Using Simple Supervised Machine Learning Methods," *Express Polymer Letters* 17, no. 9 (2023): 964–973.

[21] N. Lukács, K. E. Decsov, B. Molnár, F. Ronkay, and B. K. Bordácsné, "Increased Processing Temperature Assisted Reactive Toughening of Poly(Lactic Acid)," *Express Polymer Letters* 17, no. 2 (2023): 169–180.

[22] H. Pouriman, R. Lin, K. Graham, and K. Jayaraman, "Mechanical, Thermal and Rheological Investigation of Poly (Lactic Acid)(PLA)/Poly(3-Hydroxybutyrate-Co-Hydroxyvalerate) (PHBV) Blend Within Its Synergistic Elongation Effect Region," *Express Polymer Letters* 17, no. 4 (2023): 373–389.

[23] Y. Deng, C. Yu, P. Wongwiwattana, and N. L. Thomas, "Optimising Ductility of Poly(Lactic Acid)/Poly(Butylene Adipate-Co-Terephthalate) Blends Through Co-Continuous Phase Morphology," *Journal of Polymers and the Environment* 26, no. 9 (2018): 3802–3816.